Combined Cocurrent-Countercurrent Blowdown Cycle in Pressure Swing Adsorption

Sung-Sup Suh
Phillip C. Wankat
School of Chemical Engineering
Purdue University
West Lafayette, IN 47907

Major modifications in modern PSA (pressure swing adsorption) processes have been in the pressurization and blowdown methods. In many conventional PSA processes, the high pressure column is depressurized countercurrently. However, carrier gas is lost in the blowdown gas, and this loss increases as adsorption pressure increases. Cocurrent blowdown can be employed to reduce the loss of the carrier gas and to increase the concentration of the strong adsorbate during the blowdown step. In industrial practice (Krishnamurthy et al., 1987; Sircar and Kratz, 1988) and academic studies (Yang and Doong, 1985; Cen et al., 1985; Doong and Yang, 1986), a combined blowdown cycle where the adsorbent column is first partially depressurized cocurrently to allow for high recovery of carrier gas, and then depressurized countercurrently, is used. Kayser and Knaebel (1988) studied an integrated step of feed and cocurrent blowdown followed by countercurrent blowdown.

The four-step Skarstrom cycle was modified to repressurize the low-pressure column with high-pressure product instead of feed gas, and to add a cocurrent blowdown step prior to the countercurrent blowdown step. Accordingly, each column undergoes the following steps: pressurization with product, feed, cocurrent blowdown, countercurrent blowdown, and purge. For continuous production, two columns are interconnected to form an eight-step cycle, half of which is shown in Figure 1. The feed step continues during half of the cycle.

The purpose of this study was to determine the conditions where a combined blowdown cycle is advantageous. Both a local equilibrium model and a linear-driving-force model were used to study bulk separation of a binary gas, with uncoupled linear isotherms to determine the cocurrent blowdown pressure which maximized both recovery of the carrier gas and adsorbate enrichment.

Theory

The local equilibrium model has been used to analyze four-step cycles (Shendalman and Michell, 1972; Chan et al., 1981) and modified six-step cycles which employ repressurization with high-pressure product (Knaebel and Hill, 1985). Analysis of the cycle in this study is an extension of Knaebel and Hill (1985). The assumptions of the local equilibrium model used in this study are:

- Local equilibrium between gas and solid
- Linear equilibrium isotherms
- Negligible dispersion
- Isothermal operation
- Negligible pressure drop
- Negligible mass transfer resistance

The feed and blowdown steps are timed to prevent breakthrough of the adsorbate. Based on the local equilibrium model, the cocurrent blowdown gas is a clean carrier gas which does not include adsorbate. This gas is a light product, and if one has more than two columns or uses a compressor, the cocurret blowdown gas can be recycled to partially repressurize and/or purge other columns at low pressure and/or to be mixed with the feed gas. At the end of the cocurrent blowdown step, the column is saturated with partially desorbed adsorbate if local equilibrium is valid (there is no mass transfer zone). During the following countercurrent blowdown step, more solute is desorbed, and the solute-enriched gas is obtained as the countercurrent blowdown gas.

The numbers of moles of gas entering or leaving the column for each step are given by

$$N_{FD} = \phi \bar{P} Z_f \tag{1}$$

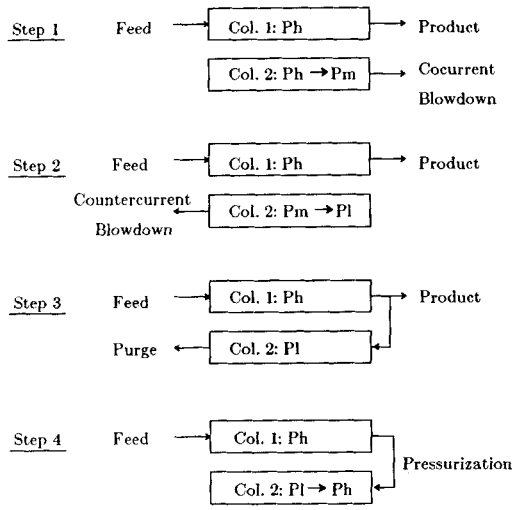

Figure 1. Half cycle of pressure swing adsorption process.

$$N_{HP} = \phi\bar{P}[1 + (\beta - 1)y_f]Z_f \tag{2}$$

$$N_{COBD} = \phi\beta P_m\left(y_f Z_f \frac{\bar{P}}{P_m} - 1\right) \tag{3}$$

$$N_{PG} = 0 \tag{4}$$

$$N_{PZ} = \phi\beta(\bar{P} - 1) \tag{5}$$

where $\phi = \epsilon V p_1/\alpha_A R_g T$; $\beta = \alpha_A/\alpha_B$ $(K_A > K_B)$; $\alpha_i = \epsilon/[\epsilon + (1 - \epsilon)K_i]$ $(i = A \text{ or } B)$; y is the mole fraction of A; $\bar{P}$ is the ratio of the high pressure to the low pressure; P_m is the ratio of the pressure at the end of the cocurrent blowdown step to the low pressure; and Z_f is the dimensionless distance of the shock wave from the feed entrance at the end of the feed step. During the cocurrent blowdown step, the characteristic position reaches the product end moving along another shock wave line. A material balance considering the shock wave before and after the cocurrent blowdown step gives

$$Z_f = \frac{y_m P_m}{y_f \bar{P}} \tag{6}$$

From the local equilibrium analysis, y_m is obtained as a function of P_m by solving

$$\frac{y_f}{(1 - y_f)^\beta}\left(\frac{\bar{P}}{P_m}\right)^{1-\beta}(1 - y_m)^\beta - y_m = 0 \tag{7}$$

Recovery of the light component in the combined process is

$$R_{comb} = \frac{N_{HP} + N_{COBD} - N_{PZ} - N_{PG}}{(1 - y_f)N_{FD}} = \left[1 - (1 - \beta)y_f + \frac{y_f}{y_m P_m}((1 - P_m)\beta - 1)\right]\Big/ (1 - y_f) \tag{8}$$

Equation 8 is easily adapted to a cycle with only cocurrent blowdown ($P_m = 1$) or only countercurrent blowdown ($P_m = \bar{P}$, $y_m = y_f$).

The usual linear-driving-force (LDF) model was solved numerically (Suh, 1988). The purpose of this exploration was to see if mass transfer resistances qualitatively changed the results. Purity and recovery of both A-rich and B-rich products and adsorbent productivity were determined, to compare the separation results. D, the dimensionless adsorbent productivity of B, was defined as the moles of B product per adsorbent weight per time (throughput of B), divided by the moles of inert gas which can be stored in the column at low pressure, per adsorbent weight per time. Separation results were compared with $D = 100 \pm 1$. This required a significant number of computer runs since D could not be set *a priori*. The inlet feed velocity and purge-to-feed ratio were varied to keep D constant. Feed gas with $\beta = 0.1$ and $y_f = 0.3$ was selected since this feed gas leads to different separation results according to the blowdown levels.

Results

The effect of P_m on recovery is shown in Figure 2 for both the local equilibrium and the linear-driving-force models. Countercurrent blowdown leads to higher recovery than the combined blowdown when P_m is low. However, the combined blowdown is preferable with higher P_m. The approximate optimum $P_m = 3$ with mass transfer is very close to the optimum P_m which was obtained in the local equilibrium model (where $y = 0$). This agreement between the models can be expected to hold when separations are based on the differences of adsorptivities instead of on the differences in the mass transfer coefficients.

Figures 3 and 4 compare recoveries calculated from the local equilibrium model for cocurrent, countercurrent and combined blowdowns as a function of the feed gas concentration, y_f. R_{comb} plotted in the figures is the value obtained at the optimum P_m. Figure 3 illustrates the case where $\beta = 0.01$. If the feed concentration is low, there is no significant difference between the recoveries. However, as y_f is increased, R_{co} decreases far below

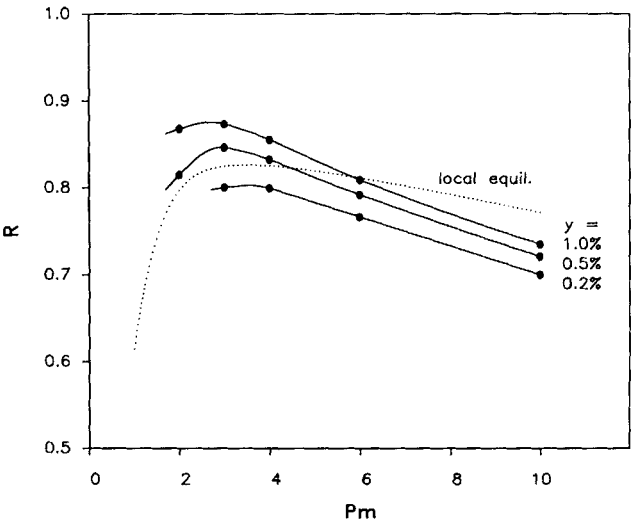

Figure 2. Recovery: local equilibrium vs. linear-driving-force model for combined cycle.

$\beta = 0.1$, $y_f = 0.3$, $\bar{P} = 10$, and $D = 100$. y = mole fraction of A in product. ($y = 0$ for local equilibrium). For comparison, $R_{counter} = 0.771$ and $R_{co} = 0.614$ from local equilibrium model.

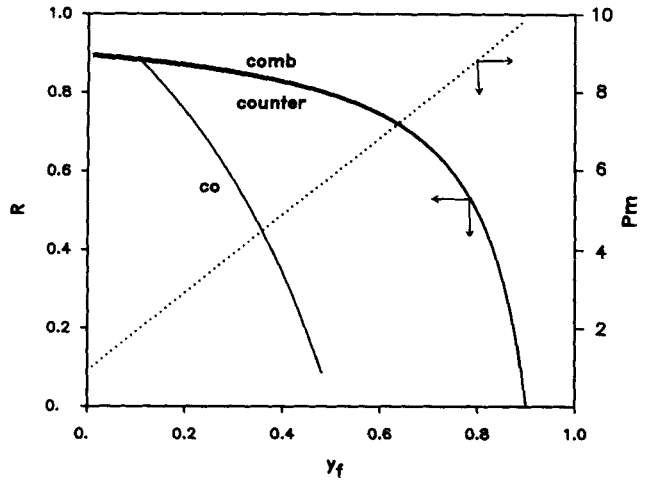

Figure 3. Local equilibrium model predictions of recoveries and optimum P_m for $\beta = 0.01$ and $\bar{P} = 10$.

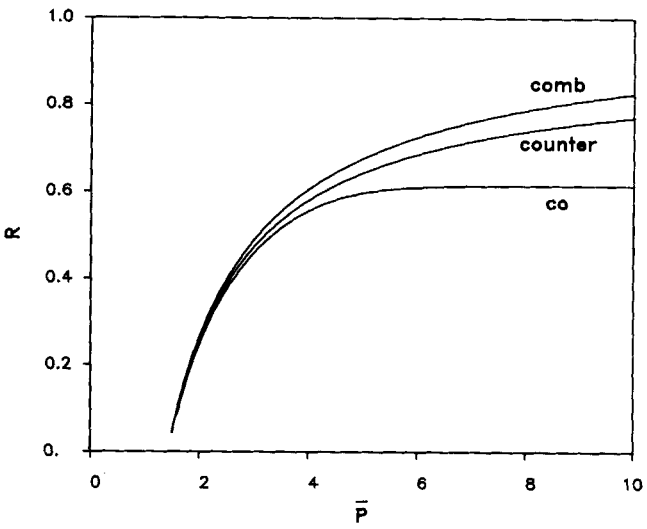

Figure 5. Local equilibrium model predictions of recoveries for $\beta = 0.1$ and $y_f = 0.3$.

the other two recoveries. R_{comb} is very close to $R_{counter}$ over the entire range of y_f. Therefore, it is not necessary to insert a cocurrent blowdown step before the countercurrent blowdown step for small β. This figure also shows that the optimum P_m increases almost linearly as y_f increases for this very low β. For the larger β value shown in Figure 4, the benefits of the combined blowdown cycle becomes significant. If y_f is smaller than 0.1, R_{comb} approaches R_{co}. If y_f is larger than 0.8, R_{comb} approaches $R_{counter}$. Kayser and Knaebel's (1988) cycle has higher R than countercurrent but lower R than the combined cycle. In Figures 3 and 4, the cocurrent blowdown cycle is shown only for limited ranges of y_f since the feasible range for contamination-free operation is severely restricted for the process with cocurrent blowdown only.

The local equilibrium model predictions of the effect of the total pressure ratio $\bar{P}$ on the recoveries and optimum P_m, are presented in Figures 5 and 6. R_{comb} and $R_{counter}$ steadily increase with the pressure ratio, while R_{co} becomes almost constant at high $\bar{P}$. Since the displacement of the characteristic position during the cocurrent blowdown step becomes larger at high $\bar{P}$ and the feed step period should be shorter, high $\bar{P}$ does not raise the recovery as much as it does in the countercurrent and combined blowdown processes. Figure 6 shows that the optimum P_m increases almost linearly with increasing $\bar{P}$. P_m increases as y_f increases and as β decreases.

Figure 7 shows the LDF model predictions of the recoveries of the light component for five blowdown pressures. For P_m less than about 4, the minimum attainable impurity increases sharply as P_m decreases, since the cocurrent product gas becomes very contaminated. Two different recoveries can be achieved with the same impurity. This multiple steady state was due to the reflux of the high-pressure product which is not impurity free. As we increased the feed velocity, purge velocity, and purge-to-feed ratio while keeping the adsorbent productivity constant, the impurity level dropped to its minimum and then increased. The same trend is shown for all P_m values in Figure 7. Therefore, operation with high gas velocities beyond the optimum point is not desirable because of low recovery and large power consumption. Additional results (Suh, 1988) show that if

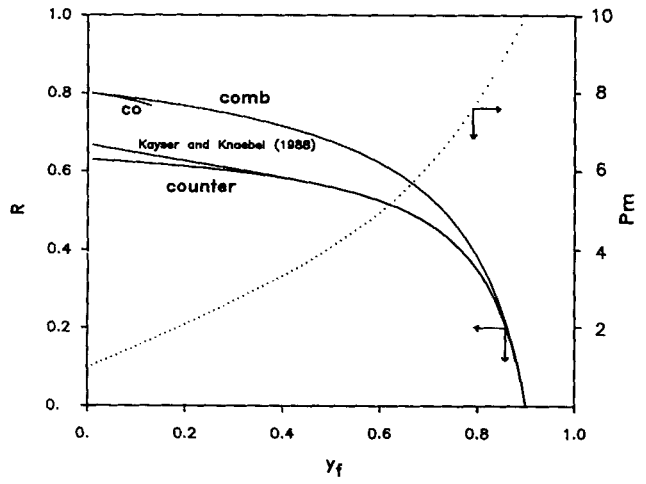

Figure 4. Local equilibrium model predictions of recoveries and optimum P_m for $\beta = 0.3$ and $\bar{P} = 10$.

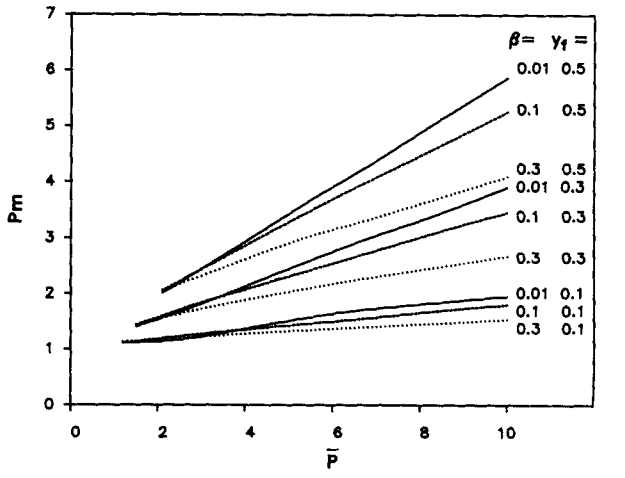

Figure 6. Local equilibrium model predictions of optimum P_m for various β and y_f.

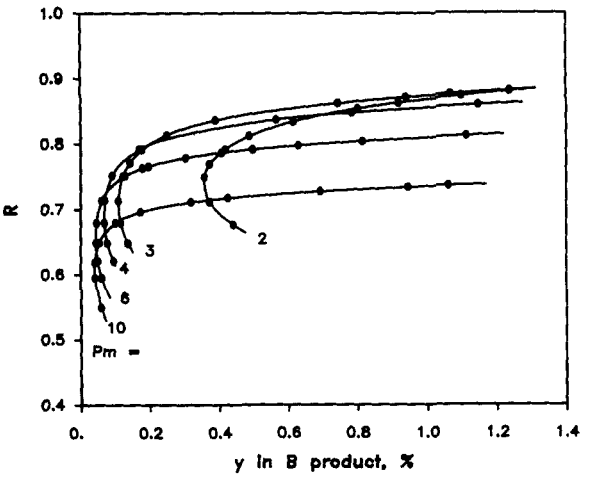

Figure 7. Linear-driving-force model predictions of recoveries vs. impurity level for various P_m. D = 100.

$\beta = 0.1$, $y_f = 0.3$ and $\bar{P} = 10$.

we reduce the adsorbent productivity without changing the recovery, we can achieve a purer product. Likewise, the minimum attainable impurity level (when recovery is of no concern) drops as the adsorbent productivity is decreased.

Discussion

The recommendations for selection of the blowdown cycle are as follows. If β is smaller than about 0.01, or y_f is larger than about 0.8, countercurrent blowdown is preferable. Otherwise, a combination of the two blowdowns is preferable for high recovery of the light component and high enrichment of the heavy component. For air separation using 5A molecular sieve, typical conditions are $\beta = 0.6$ (Kayser and Knaebel, 1986) and $y_f = 0.79$. Since the feed concentration is high, cocurrent blowdown is not recommended. In the case of hydrogen purification using activated carbon where methane is an impurity, the combination of two blowdowns is effective since $\beta = 0.18$ (Sircar and Kumar, 1983), and y_f is typically less than 0.7 (often much less). In the case of air drying on silica gel, cocurrent blowdown is not recommended, since $\beta \ll 0.001$ (Carter and Wyszynski, 1983).

The cocurrent blowdown step produces pure product at low pressure, which may require additional compression. Moreover, it may not be easy to accurately control the pressure change during the blowdown. The combined-blowdown process is recommended only when there is a distinct increase in the recovery.

The optimum P_m which is obtained from the linear-driving-force model for any impurity level is close to that derived from the local equilibrium model. In order to search for the optimum P_m using the mass transfer model, many calculations were required in order to keep the adsorbent productivity constant. Therefore, it is advantageous to first predict the optimum P_m with the local equilibrium model, and then to use a mass transfer model or experiments.

Acknowledgement

This research was partially supported by the National Science Foundation under grant CBT-8520700.

Notation

D = adsorbent productivity
K_i = linear equilibrium distribution coefficient of component i
N = moles of gas entering or leaving column during the step designated by subscript, gmol
p_h = pressure during feed step, atm
p_l = pressure during purge step, atm
p_m = pressure at the end of cocurrent blowdown, atm
$\bar{P} = p_h/p_l$
$P_m = p_m/p_l$
R = fractional recovery of B
R_g = gas constant, 82.06 cm^3 · atm/gmol · K
T = absolute temperature, K
V = column volume, cm^3
y = mole fraction of heavy component A in gas phase
y_f = y in feed
y_m = y at the end of cocurrent blowdown step
Z = axial distance in the column
Z_f = displacement of shock wave during feed step

Greek letters

α_i = ratio of voids to total i, $\epsilon/[\epsilon + (1-\epsilon)K_i]$
β = relative separation factor, α_A/α_B for $K_A > K_B$
ϵ = column void fraction
ϕ = moles A in saturated column at p_l, $\epsilon V_{p_l}/\alpha_A R_g T$

Subscripts

A = heavy component ($K_A > K_B$)
B = light component
co = cocurrent-blowdown process
$comb$ = combined-blowdown process
$counter$ = countercurrent-blowdown process
$COBD$ = cocurrent blowdown
FD = feed
HP = high-pressure production
PG = purge
PZ = repressurization

Literature cited

Carter, J. W., and M. L. Wyszynski, "The Pressure Swing Adsorption Drying of Compressed Air," *Chem. Eng. Sci.*, **38**(7), 1093 (1983).

Chan, Y. N. I., F. B. Hill, and Y. W. Wong, "Equilibrium Theory of a Pressure-Swing Adsorption Process," *Chem. Eng. Sci.*, **36**, 243 (1981).

Cen, P.-L., W.-N. Chen, and R. T. Yang, "Ternary Gas Mixture Separation by Pressure Swing Adsorption: A Combined Hydrogen-Methane Separation and Acid Gas Removal Process," *Ind. Eng. Chem. Proc. Des. Dev.*, **24**, 1201 (1985).

Doong, S.-J., and R. T. Yang, "Bulk Separation of Multicomponent Gas Mixtures by Pressure Swing Adsorption: Pore/Surface Diffusion and Equilibrium Models," *AIChE J.*, **32**(3), 397 (1986).

Kayser, J. C., and K. S. Knaebel, "Pressure Swing Adsorption: Experimental Study of an Equilibrium Theory," *Chem. Eng. Sci.*, **41**(11), 2931 (1986).

Kayser, J. C., and K. S. Knaebel, "Integrated Steps in Pressure Swing Adsorption Cycles," *Chem. Eng. Sci.* **43**(11), 3015

Knaebel, K. S., and F. B. Hill, "Pressure Swing Adsorption: Development of an Equilibrium Theory for Gas Separations," *Chem. Eng. Sci.*, **40**(12), 2351 (1985).

Krishnamurthy, R., Y. Shukla, and D. L. MacLean, "High Yield HARP Plant for Argon Recovery from Ammonia Purge Gas," AIChE meeting, Minneapolis, (Aug., 1987).

Shendalman, L. H., and J. E. Mitchell, "A Study of Heatless Adsorption on the Model System CO_2 in He," *Chem. Eng. Sci.*, **27**, 1449 (1972).

Sircar, S., and W. C. Kratz, "A Pressure Swing Adsorption Process for Production of 23–50% Oxygen-Enriched Air," *Sep. Sci. Technol.*, **23**, 437 (1988).

Sircar, S., and R. Kumar, "Adiabatic Adsorption of Bulk Gas Mixtures: Analysis by Constant Pattern Model," *Ind. Eng. Chem. Proc. Des. Dev.*, **22**, 271 (1983).

Suh, S.-S., PhD Thesis, Purdue Univ., West Lafayette, IN (1988).

Yang, R. T., and S.-J. Doong, "Gas Separation by Pressure Swing Adsorption: A Pore Diffusion Model for Bulk Separation," *AIChE J.*, **31**, 1829 (1985).

Manuscript received July 18, 1988 and revision received Oct. 20, 1988.